Journal of Biomechanics 49 (2016) 3592–3595

Contents lists available at ScienceDirect

Journal of Biomechanics

journal homepage: www.elsevier.com/locate/jbiomech
www.JBiomech.com

Short communication

Influence of intramuscular fiber orientation on the Achilles tendon curvature using three-dimensional finite element modeling of contracting skeletal muscle

Ryuta Kinugasa [a,*,1], Naoto Yamamura [b,1], Shantanu Sinha [c], Shu Takagi [b]

[a] Department of Human Sciences, Kanagawa University, Japan
[b] Department of Mechanical Engineering, The University of Tokyo, Japan
[c] Department of Radiology, University of California, San Diego, USA

ARTICLE INFO

Article history:
Accepted 12 September 2016

Keywords:
Muscle contraction
Finite element analysis
Tendon curvature
Fiber pennation angle
Achilles tendon

ABSTRACT

Tendon curvature plays a key role in mechanical gain (amplifying the joint excursion relative to fiber length change) during joint motion, but the mechanism remains unresolved. A three-dimensional finite element (FE) model was used to investigate the influence of intramuscular fiber orientation upon the curvature pattern of the Achilles tendon during active muscular contraction. Two simulation models, with fiber pennation angles of $\theta = 25^\circ$ and 47° were tested for the gastrocnemius and soleus muscles. A smaller pennation angle (25°) of the soleus muscle fibers was accompanied by a large change in curvature whereas a larger pennation angle (47°) of the soleus muscle was accompanied by small effects. These results suggest that the fiber pennation angle determines the curvature of the tendon, and the magnitude of the curvature varies along the length of the aponeurosis. Such FE modeling has the potential of determining changes in force output consequent to changes in intramuscular fiber orientation arising from resistance training or unloading, and provides mechanism for predicting the risk of Achilles tendon ruptures.

1. Introduction

Muscles act in series with tendons which are characterized by their elastic properties. Tendon elasticity provides a variety of important functions during movement (Roberts and Azizi, 2011). The tendons also play a key role in mechanical gain during joint motion that cannot be solely attributed to tendon elasticity (Csapo et al., 2013). There has to be some mechanisms for amplifying the joint excursion relative to fiber length changes by tendon curvature (Csapo et al., 2013; Hodgson et al., 2006). A curvature would act to prevent outward movement of the tendon as the joint rotates, but possible mechanisms that would cause the bending of the tendon remain unresolved.

Recent work, using a finite element model (FEM) has hinted at such possible mechanisms of the tendon curvature, with muscle bulging with different pennation angles under isometric contraction (Hodgson et al., 2012). One implication of such findings is that tendon curvature can influence the motion of the muscle associated with muscle fiber orientation.

The hypothesis that is being tested, utilizing a three-dimensional FEM investigation, is that intramuscular fiber orientation i.e. fiber pennation angles with the aponeurosis, influences the changes in tendon curvature during active contraction. Since it is difficult to identify such anatomical structure or mechanism involved even through *in vivo* human experimental study, our objective was to develop computational models of skeletal muscle and tendon, the results of which can yield better understanding of how the tissue organization and mechanics result in the observed curvature of the Achilles tendon and help identify possible candidate mechanisms contributing to this curvature. Our findings will clarify the importance of individual intramuscular structural materials and offer possible clues about the importance of the tendon's line of action or excursion of the calcaneus.

2. Methods and materials

In order to generate the 3-dimensional finite-element (FE) mesh described in the next paragraph, images of the relevant human anatomy was acquired from a single male subject (age 25 years; height 170 cm; weight 60 kg), with signed informed consent to participate in an Institutional Review Board approved study. The subject was imaged in the supine position with a 1.5-T magnetic resonance

* Correspondence to: Department of Human Sciences, Kanagawa University, 3-27-1 Rokkakubashi, Kanagawa-ku, Yokohama, Kanagawa 2218686, Japan.
Fax: +81 45 481 5670.
E-mail address: rk@kanagawa-u.ac.jp (R. Kinugasa).
[1] R. Kinugasa and N. Yamamura contributed equally to this work.

http://dx.doi.org/10.1016/j.jbiomech.2016.09.014
0021-9290/

scanner (Exelart, Toshiba Medical Systems, Tochigi, Japan). A series of axial-plane MR images were acquired from the patella to the calcaneus bone with 3 mm slice thickness (matrix 256 × 256; field of view, 256 × 256 mm^2) and 0 mm slice interval (i.e. the acquired slices were contiguous).

The muscle, connective tissue, and bone were manually outlined using indigenously developed segmentation software (RV-Editor, RIKEN, Saitama, Japan). The process for building the FE model has been described previously (Yamamura et al., 2014). Briefly, FE meshes were constructed including 8 hexahedral elements and 76,862 nodes. The element size was reduced to the minimum required to detect a difference in the tendon curvature among the four Cases described below. The meshes consisted of two materials – triceps surae muscles [gastrocnemius and soleus (Sol) muscles] and Achilles tendon with proximal aponeurosis – connected rigidly by coincident nodes. Muscle and connective tissue were modeled as transversely isotropic, hyperelastic, and quasi-incompressible. A Hill-type model was adopted to simulate muscle contraction (Johansson et al., 2000). The constitutive formulation has previously been described in detail (Yamamura et al., 2014). The bones of the lower limb, based on data reported in the literature (Delp et al., 1990), were modeled as rigid bodies, and the ankle joint was modeled as a frictionless pin joint. The coordinates of the Achilles tendon insertion to the calcaneal tuberosity and the pin joint of ankle were obtained from the 3D lower limb musculoskeletal model (Delp et al., 1990).

We generated a representation of the three-dimensional geometry of fibers within each of the two muscles, the gastrocnemius and the Sol, using a mapping technique that applies fiber geometry to the FE mesh. We produced a fiber map that consisted of a set of interpolated cubic splines (Fig. 1B). For each element in the mesh, we defined the reference fiber based on fascicle orientation measurements from ultrasound images (Kawakami et al., 1998). The fiber direction was determined as the vector tangent to the spline curve at the reference fiber. The fiber pennation angle was set at each material point (Gauss point) of the finite elements. Two simulation models, with fiber pennation angles of $\theta = 25°$ and 47° were considered (Fig. 2A). These two pennation angles were chosen since they represent the range of pennation angles encountered in normal muscle activities as reported in the literature (Maganaris et al., 1998; Kinugasa et al., 2013) and also to study if pennation angle has a significant impact on tendon curvature. The permutations of the two muscles with the two angles of pennation lead to four cases are shown as Cases 1, 2, 3 and 4 that were investigated in this study (Table 1).

The simulations were performed with the ankle angle at 90° of the foot. We prescribed a value of 0.1 (10% maximum voluntary activation) for the activation level in all the muscles, for the simulation results presented in this study. This 10% activation level was chosen since this is about the maximum intensity at which the tendon can be curved in our FE model. Because the model we have used herein is deliberately a very simple one, with minimal assumptions (such as the exclusion of surface skin, subcutaneous fat, connective tissues such as fascia and epimysium, as well as the antagonist muscle components), the tendon achieved the maximum curvature, and the ankle moved from its initial state to the fully plantarflexed position at a relatively small 10% activation level. However, with this simple model with minimum assumptions, we were able to gain some insight into the potential importance of muscle architecture properties on the tendon curvature. We used this configuration of tendon and foot and this activation level for the rest of our simulations. To quantify tendon curvature, 705 points were positioned along a representative Achilles tendon from the most proximal, the muscle-tendon junction (MTJ) to the most distal end at the calcaneus (Appendix A). These served as nodes for the FE simulation. Further, in order to test the effect of element size on the tendon curvature, the MTJ to calcaneous was sub-divided 2, 4, 8, 16 and 32 fold. Based on these results, every 3rd nodes in this series was used to calculate the curvature using Eq. (1) in Appendix A.

3. Results

The three-dimensional FEM investigation yielded the curvature distribution along the entire Achilles tendon during 10% muscle activation, as a function of the change in fiber pennation angle with the aponeurosis between the four different Cases 1 to 4. The results of this validation of our hypothesis, stated in the Introduction was plotted in Fig. 2B.We tested the effect of element size on the curvature of the Achilles tendon: a 16 and 32-fold resolution yielded a well-converged, smooth curve. Hence a 32-fold resolution was used for the sub-division of the tendon along the proximodistal direction

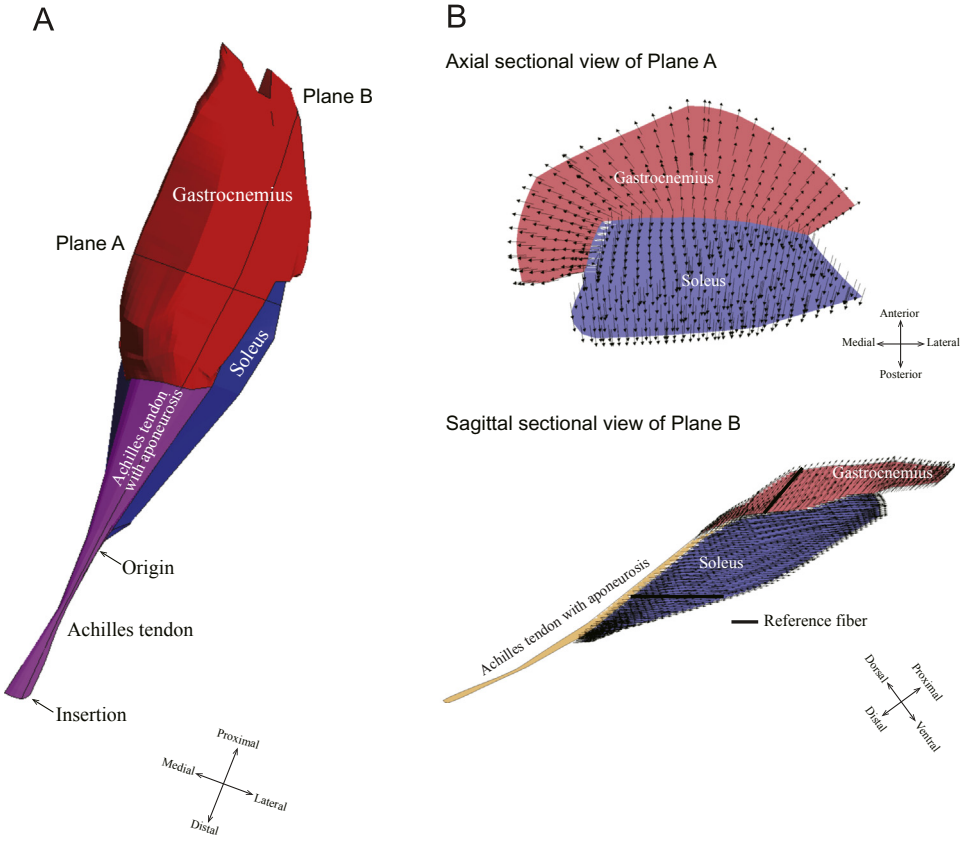

Fig. 1. Diagram of the basic model. A: Three-dimensional finite element model that involves the triceps surae muscles, Achilles tendon with proximal aponeurosis, and bones. Achilles tendon with proximal aponeurosis are overlaid on the surface portion of the Soleus muscle and connected to the calcaneus. The initial muscle fiber length corresponded to the length at which the passive materials were in their neutral position. The orientation of the Plane A is shown by horizontal line in the gastrocnemius and Soleus muscles. Similarly, the orientation of the Plane B is shown by vertical line from the gastrocnemius muscle to the insertion of the Achilles tendon. B**:** Fiber map geometry representing the gastrocnemius and soleus muscles. Representative muscle fibers were mapped through the FE mesh to define initial fiber direction at each element (reference fiber drawn as thick line in the sagittal sectional view of Plane B). A small arrow in the each muscle indicates the orientation of the fiber.

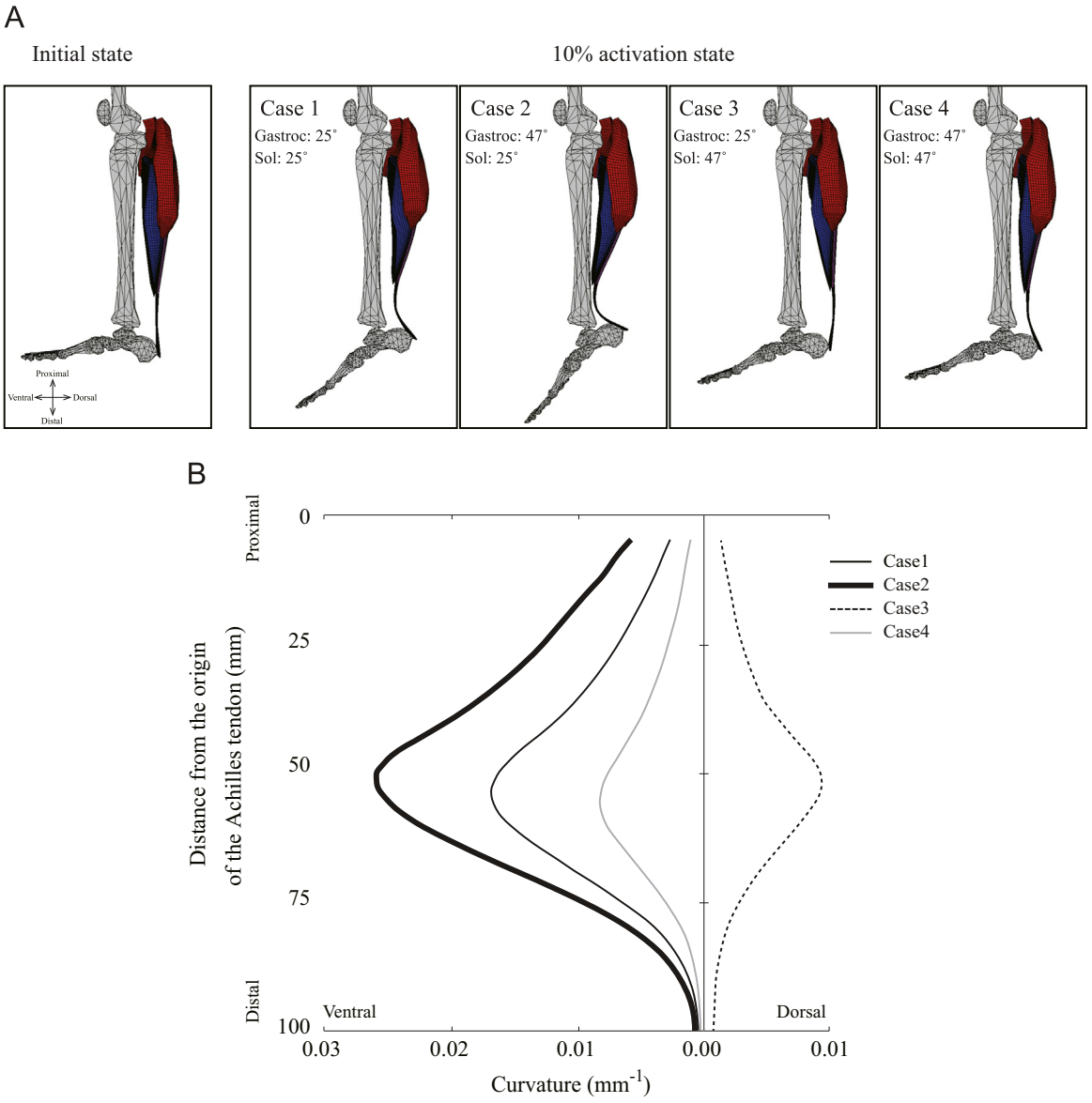

Fig. 2. The effect of fiber pennation angle on the curvature of the Achilles tendon under 10% muscle activation using three-dimensional finite element modeling. A: Four models were tested; the fibers were arranged at a pennation angle of 25° or 47° for the gastrocnemius (Gastroc) and soleus (Sol) muscles, respectively (further clarified in Table 1). Simulation of triceps surae muscles with fibers at 25° or 47° when the muscles were allowed to move freely between fixation points at the ends of the tibia and calcaneal bone. B: Comparison of the curvature variation along the Achilles tendon in response to a 10% activation level for all 4 cases. The distance 0 mm was identified as the origin of the Achilles tendon, whereas the distance 100 mm was identified as the insertion to the calcaneal tuberosity. The three solid lines for the Case 1, 2, and 4 illustrate the curvature towards the ventral direction while the dotted line for the Case 3 illustrates the curvature towards the dorsal direction.

Table 1
Description of cases in terms of muscle type and pennation angle.

	Gastroc	Sol
Case 1	25°	25°
Case 2	47°	25°
Case 3	25°	47°
Case 4	47°	47°

Value: pennation angle (°).
Gastroc; gastrocnemius, Sol; soleus.

for all further calculations. A progressive increase in curvature towards the ventral direction in the dorsoventral plane, from the origin to the opposite extremity of the insertion of the Achilles tendon was found for Cases 1, 2, and 4. In these three cases, the distal end of the Sol muscle shifted anteriorly compared to the calcaneus. The reverse of this trend was observed in Case 3 with a dorsal movement of the distal end of the Sol muscle along the dorsoventral axis. Case 2 exhibited the largest curvature, which corresponds to the distal end of contracted Sol muscle moving the most towards the anterior side with respect to the calcaneus compared to Cases 1 and 4.

4. Discussion

A potential mechanism for the pennate muscle-induced curvature of the Achilles tendon is being proposed here. This model was developed to simulate for the first time, the effect of the fiber pennate arrangement of the triceps surae muscle on the Achilles tendon curvature. Our hypothesis stated in the Introduction was validated in that the FE analysis confirmed that the pennation angle of the muscle fibers influence on the Achilles tendon curvature. Fiber pennate

arrangement plays an important role in the final resultant motion of a muscle. This is especially true if one end of the fiber is attached to underlying tissues to add to the displacement resulting from the angular arrangement of the fibers. This mechanism is basically the same as the mechanism by which the intercostal muscles raise the rib cage during respiration, which was first discovered more than 250 years ago (Hamberger, 1749). The pennate arrangement of the muscle fibers results in each end of different fibers exerting a different force at different points along the muscle, generating a turning moment that is canceled by the action of other fibers, except at the ends of the muscle. Thus, the overall action of the Sol fibers is to rotate the Achilles tendon towards the tibia, whereas the gastrocnemius fibers rotate the tendon away from the tibia.

A single subject was scanned for this study in order to acquire images of the anatomy spanning the entire 3-dimensional extent of the lower leg and generate the three-dimensional FE mesh. Since no parameter was been measured that required statistical averaging, a single subject rather than a cohort sufficed for the purpose. Our FE analysis confirmed that a smaller pennation angle of the Sol muscle leads to a greater magnitude of curvature change. A smaller pennation angle implies a greater distance between the muscle fiber origin and insertion; thus, the overall muscle deformation is greater at a smaller pennation angle. This prediction seems consistent with the magnitude of the curvature relative to the pennation angles of the Sol and gastrocnemius muscles (Fig. 2B). It is possible that the passive tension of the fibers has some effect. However, our FE model seems to indicate empty space between the Sol muscle and tibia, which would not pose any hindrance to the movement of the Sol muscle. This is of course not the case in an actual human leg, in which the tissues between the Sol and tibia would prevent movement, in which case the large tendon curvature we found might not be so pronounced.

The question remains as to why Case 3 yields a completely opposite sign of curvature in the Achilles tendon compared to Cases 1, 2 and 4. Although mechanical constraints on the outward movement of the Achilles tendon may be postulated to be the presence of the surface skin, this can be more likely explained by a bulging direction (Kinugasa et al., 2012) depending upon fiber pennation angle. Smaller pennation angles of the gastrocnemius fibers favored a dorsally bulge with a large magnitude while larger pennation angles of the Sol fibers favored a ventral bulge with a small magnitude, suggesting the gastrocnemius deformation must be greater than the Sol deformation. Consequently, the Achilles tendon deformed away from the tibia.

A major goal of this paper was to identify the critical features which could significantly influence the Achilles tendon behavior. Our first consideration was therefore to understand how the pennation angle impacts the Achilles tendon bending. We have deliberately used very simple models with minimal assumptions, to gain some insight of the potential importance of muscle architecture properties. The experimental observations showing that the Achilles tendon bend in the ventral direction with smaller pennation angles (as seen in human) in contracting human plantarflexors (Csapo et al., 2013) is reproduced in the current FE model. The Achilles tendon model is based on published model in our previous study (Yamamura et al., 2014). The material properties in this model employs values within the range of experimental data (Louis-Ugbo et al., 2004; Reeves et al., 2005; Rosager et al., 2002; Shin et al., 2008). Nevertheless, the Achilles tendon force computed by this model (approximate 600 N) differ a two-fold range with experimental data (approximate 1300 N) (Yamamura et al., 2014).

Author contributions

Conception and design of the study; RK, NY, SS, Acquisition and analysis of data; RK, NY, Contributed new reagents/analytic tools; NY, ST, Interpretation of data; RK, NY, ST, drafting the article; RK, revising it critically for important intellectual content; RK, NY, SS, ST, final approval; RK, NY, SS, ST.

Competing interests

No conflicts of interest, financial or otherwise, are declared by the authors.

Acknowledgments

We thank J. A. Hodgson for discussions on data. This study was supported by HPCI Strategic Programs for Innovative Research Field 1 "Supercomputational Life Science" by MEXT (to S.T.) and Japan Society for the Promotion of Science (JSPS) Grant-in-Aid for Scientific Research (KAKENHI) (C) 2535082 (to R.K.).

Appendix A. Supporting information

Supplementary data associated with this article can be found in the online version at http://dx.doi.org/10.1016/j.jbiomech.2016.09.014.

References

Csapo, R., Hodgson, J., Kinugasa, R., Edgerton, V.R., Sinha, S., 2013. Ankle morphology amplifies calcaneus movement relative to triceps surae muscle shortening. J. Appl. Physiol. 115, 468–473.

Delp, S.L., Loan, J.P., Hoy, M.G., Zajac, F.E., Topp, E.L., Rosen, J.M., 1990. An interactive graphics-based model of the lower extremity to study orthopaedic surgical procedures. IEEE Trans. Biomed. Eng. 37, 757–767.

Hamberger, G.E., In: Hamberger, G.E. (Ed.), De Respirationis Mechanismo et usu genuine. 1749 Croeker, Jenae, pp. 1–182

Hodgson, J.A., Finni, T., Lai, A.M., Edgerton, V.R., Sinha, S., 2006. Influence of structure on the tissue dynamics of the human soleus muscle observed in MRI studies during isometric contractions. J. Morphol. 267, 584–601.

Hodgson, J.A., Chi, S.W., Yang, J.P., Chen, J.S., Edgerton, V.R., Sinha, S., 2012. Finite element modeling of passive material influence on the deformation and force output of skeletal muscle. J. Mech. Behav. Biomed. Mater. 9, 163–183.

Johansson, T., Meier, P., Blickhan, R., 2000. A finite-element model for the mechanical analysis of skeletal muscles. J. Theor. Biol. 206, 131–149.

Kawakami, Y., Ichinose, Y., Fukunaga, T., 1998. Architectural and functional features of human triceps surae muscles during contraction. J. Appl. Physiol. 85, 398–404.

Kinugasa, R., Hodgson, J.A., Edgerton, V.R., Sinha, S., 2012. Asymmetric deformation of contracting human gastrocnemius muscle. J. Appl. Physiol. 112, 463–470.

Kinugasa, R., Oda, T., Komatsu, T., Edgerton, V.R., Sinha, S., 2013. Interaponeurosis shear strain modulates behavior of myotendinous junction of the human triceps surae. Physiol. Rep. 1, e00147.

Louis-Ugbo, J., Leeson, B., Hutton, W.C., 2004. Tensile properties of fresh human calcaneal (Achilles) tendons. Clin. Anat. 17, 30–35.

Maganaris, C.N., Baltzopoulos, V., Sargeant, A.J., 1998. In vivo measurements of the triceps surae complex architecture in man: implications for muscle function. J. Physiol. 512, 603–614.

Reeves, N.D., Maganaris, C.N., Ferretti, G., Narici, M.V., 2005. Influence of 90day simulated microgravity on human tendon mechanical properties and the effect of resistive countermeasures. J. Appl. Physiol. 98, 2278–2286.

Roberts, T.J., Azizi, E., 2011. Flexible mechanisms: the diverse roles of biological springs in vertebrate movement. J. Exp. Biol. 214, 353–361.

Rosager, S., Aagaard, P., Dyhre-Poulsen, P., Neegaard, K., Kjaer, M., Magnusson, S.P., 2002. Load-displacement properties of the human triceps surae aponeurosis and tendon in runners and non-runners. Scand. J. Med. Sci. Sport. 12, 90–98.

Shin, D., Finni, T., Ahn, S., Hodgson, J.A., Lee, H.D., Edgerton, V.R., Sinha, S., 2008. Effect of chronic unloading and rehabilitation of human Achilles tendon properties: a velocity-encoded phase-contrast MRI study. J. Appl. Physiol. 105, 1179–1186.

Yamamura, N., Alves, J.L., Oda, T., Kinugasa, R., Takagi, S., 2014. Effect of tendon stiffness on the generated force at the Achilles tendon–3D finite element simulation of a human triceps surae muscle during isometric contraction. J. Biomech. Sci. Eng. 9, 13–00294.